

Properties of Convex Optimal Power Flow Model for Meshed Power Networks

Zhao Yuan, *Member, IEEE*, Mario Paolone, *Senior Member, IEEE*

Abstract—In this paper, we firstly discuss the reduction of the approximation gap of the convex optimal power flow (OPF) model based on the branch flow formulation by deriving branch ampacity constraint associated to power losses. This new derivation of the branch ampacity constraint is because of the correct physical interpretation of the transmission line Π -model and practical engineering considerations. We rigorously prove or derive: (i) the approximated voltage phase angle constraint, required to make the branch flow model valid for both radial and meshed power networks, is a relaxation of the original nonconvex AC optimal power flow (o-ACOPF) model; (ii) necessary conditions to recover a feasible solution of the o-ACOPF model from the optimal solution of the convex second-order cone ACOPF (SOC-ACOPF) model; (iii) the expression of the global optimal solution of the o-ACOPF model providing that the relaxation of the SOC-ACOPF model is tight; (iv) the (parametric) optimal value function of the ACOPF or SOC-ACOPF model is monotonic with regarding to load absorptions if the objective function is monotonic with regarding to the nodal power injections; (v) tight solutions of the SOC-ACOPF model always exist when load absorptions become sufficiently large. Numerical simulations for various power networks to validate our analytical proofs are given and discussed.

Index Terms—Optimal Power flow, ampacity constraint, tight solution, second-order cone programming.

I. INTRODUCTION

OPTIMAL power flow (OPF) is a fundamental mathematical optimization model for decision making in power system operation and planning [1]. Improving the solution quality of OPF can give large economic and engineering benefits to the power industry [2], [3]. Recent literature focusing on the convexification of the OPF model suffered from inexactness due to the relaxation of several constraints [4]–[14]. The branch flow formulation of the power flow equations for radial power networks has been originally derived by Baran and Wu in [15] to optimize the placement of capacitor in radial distribution networks. In [16], Jabr derives a conic programming approach to solve load flow in radial distribution network. In [4], Farivar and Low propose the branch flow model as a relaxed OPF model by relying on second-order cone programming (SOCP) and prove that the relaxation is tight for radial networks under the assumption that the upper bound of power generation is infinite. In [5], Gan, Li et al. prove that the optimal solution of the branch flow model is exact (tight) if the voltage upper bounds are not binding and the network parameters satisfy some mild conditions which can be checked *a priori*. Christakou, Tomozei et al. show in [17] that the branch flow model is not exact due to the approximation

of the ampacity constraint of the branch. Nick et al. propose an exact convex OPF model for radial distribution networks in [18] by considering the shunt parameters associated to the exact modelling of the lines or other branch elements. Sufficient conditions regarding the network parameters under which the convex OPF model in [18] can give exact solutions to the original ACOPF are provided and rigorously proved. In [6], Kocuk, Dey et al. propose three methods (arctangent envelopes, dynamic linear inequalities and separation over cycle constraints) to strengthen or tighten SOCP relaxation of OPF. Numerical results show better solution quality of SOCP-based model over SDP-based model [6].

Semidefinite programming (SDP) relaxation of OPF has been firstly proposed by Bai et al. in [7]. The proposed procedures derive the rectangular form OPF in a quadratic programming model and replace the variable-vector (\mathbf{x}) by the variable-matrix ($X = \mathbf{x}^T \mathbf{x}$). Solutions of OPF can be recovered from the square roots of the diagonal elements in the variable-matrix [7]. SDP advantages in avoiding the derivation of Jacobian and Hessian matrices if the interior point method (IPM) is used [7]. Lavaei and Low propose to solve the SDP relaxation of the dual OPF problem [8]. They prove that sufficient and necessary condition of zero duality gap holds for several IEEE test cases (14, 30, 57, 118) at the the base power load levels.¹ But the branch ampacity constraint is not fully addressed. Especially, as it is proved in [17], [18], the physical interpretation of the transmission line Π model is not correct in [8]. In [19], Madani, Sojoudi et al. show that SDP relaxation works well if the line capacity is expressed by nodal voltage variables. A penalization method is proposed in [19] to reduce the rank of the SDP solution. Recently, Eltvéd, Dahl et al. numerically investigate the computational efficiency of SDP by using test cases up to 82,000 nodes which is solved in around 7 hours using a high performance computing node [20]. Based on polynomial optimization theory, Molzahn and Hiskens propose the moment-based relaxations of OPF in [9]. This formulation firstly defines order- γ moment relaxation x_γ of all monomials \hat{x}^α of voltage real-and-imaginary components \hat{x} . Then, all the monomials \hat{x}^α up to order 2γ constitute the symmetric moment matrix M_γ which is used to re-formulate the OPF constraints via the SDP. Global optimal solutions are found, at the cost of heavy computational burden due to higher relaxation order γ , for the test cases in [9]. The same authors in [10] improve the computational efficiency of this method by exploiting power system sparsity and applying high relaxation order to specific buses. In [11], Hijazi, Coffrin et al. propose a

Z. Yuan and M. Paolone are with the Distributed Electrical Systems Laboratory of École polytechnique fédérale de Lausanne (EPFL), Lausanne, 1015, Switzerland. Email: zhao.yuan@epfl.ch, mario.paolone@epfl.ch

¹As a comparison, in this paper, we evaluate the OPF solutions of test cases at low power load levels (for which the relaxation gaps are prominent).

quadratic convex (QC) relaxation by replacing the nonconvex voltage-amplitude-and-phase-angle associated constraints with the corresponding convex envelopes. In [12], the same authors investigate the relationships between different convex OPF formulations including QC, SDP and SOCP. Reducing the optimality gap of QC or SOCP based OPF models by bound tightening techniques can be found in [13], [14]. Recently, Shchetinin et al. propose in [21] three methods which require solving optimization problems to tighten the upper bounds of the voltage phase angle difference in order to satisfy the branch ampacity constraint. The same authors in [22] propose an iterative algorithm to construct a number of linear constraints (based on inner or outer approximation) to approximate the branch ampacity constraint.

In this paper, we focus on the formal derivation of equivalent ampacity constraint for the branch power losses. More specifically, we consider to improve the convex OPF in meshed power networks which necessitates the additional voltage phase angle constraint. Instead of using the approach in [18] to reformulate the branch flow model, we keep using the same set of variables (in the form of power flow variables) of the branch flow model but equivalently derive the ampacity constraint for the power losses. In this way, we overcome the approximation gap due to neglecting of the shunt elements of the branches. We then propose six theorems explaining important properties of the proposed SOC-ACOPF model. In this regard, the main contributions of this paper are: (i) derivation of the equivalent branch ampacity constraint for the power losses; (ii) proving that the SOC-ACOPF model (with additional constraint to improve its feasibility according to the original ACOPF constraints) is a relaxed ACOPF model; (iii) deriving a feasible solution recovery procedure when the SOC relaxation is tight; (iv) demonstrating that the (parametric) optimal value functions of the SOC-ACOPF model and o-ACOPF model are monotonic with regarding to nodal load absorptions when the objective function is monotonic with regarding to nodal power injections; (v) explaining that larger load absorptions can tighten the relaxation in the SOC-ACOPF model. The rest of this paper is organized as follows. Section II formulates the o-ACOPF model and SOC-ACOPF model for meshed power networks. Section III derives the equivalent branch ampacity constraint for power losses. Section IV proposes and proves important properties of the SOC-ACOPF model. Section V gives the numerical validations of our analytical proofs and discussions. Section VI concludes.

II. OPTIMAL POWER FLOW MODEL

A. Power based Branch Flow Model

We assume that the three-phase power grid satisfies two conditions: (i) all the branches and shunt impedances are circularly symmetric; (ii) all the triplets of nodal voltages and branch currents are symmetrical and balanced. These two conditions validate the use of single-line equivalent model of the three-phase power grid. The full ACOPF model is based on the validated branch flow model presented in [23]. We denote this original ACOPF model as o-ACOPF model-(1). The variable convention makes reference to the branch II-model

in Fig. 1. X_l, R_l are the longitudinal reactance and resistance of branch l . B_{s_l}, B_{r_l} are the sending- and receiving-end shunt susceptance of branch l . v_n is the phase-to-ground voltage magnitude at node n . p_{s_l}, q_{s_l} are the non-measurable sending-end active and reactive power flows for branch l . p'_{s_l}, q'_{s_l} are the measurable sending-end active and reactive power flows for branch l . p_{r_l}, q_{r_l} are the non-measurable receiving-end active and reactive power flows of branch l . p'_{r_l}, q'_{r_l} are the measurable receiving-end active and reactive power flows of branch l . q_{cs_l}, q_{cr_l} are the sending- and receiving- end shunt reactive power of branch l . The subscripts s, r, d, o in $p_{\cdot}, q_{\cdot}, v_{\cdot}, V_{\cdot}, p_{\cdot}, q_{\cdot}$ are not indices but imply the meaning of sending-end of branch l , receiving-end of branch l , load absorptions and power losses, correspondingly.

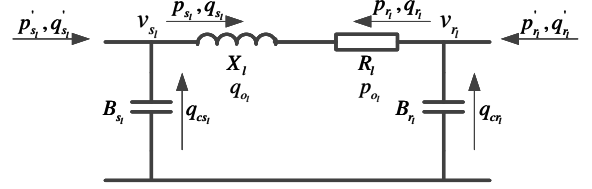


Fig. 1. The branch II-model and associated variables

Note $(p'_{s(r)l}, q'_{s(r)l})$ are the actual (i.e. measurable) branch power flows. The variables $(p_{s(r)l}, q_{s(r)l})$ are the non-measurable branch power flows used in our OPF model. For the differences between $(p'_{s(r)l}, q'_{s(r)l})$ and $(p_{s(r)l}, q_{s(r)l})$, or between $i'_{s(r)l}$ and $i_{s(r)l}$, please refer to references [17] and [18]. We want to emphasize here that the physical interpretation of the branch II-model is very important since the phase-to-ground capacitance is actually distributed along the branch which means the current (or power) flowing through the branch is actually not the same along the branch due to the charging current (or power) flowing from the distributed phase-to-ground capacitance. This means the actual power flow variables p_{s_l}, q_{s_l} is non-measurable and difficult to be constrained. This is the major reason we can only use the measurable power flow variables p'_{s_l}, q'_{s_l} to constrain the branch ampacity then derive the relationship between $(p'_{s(r)l}, q'_{s(r)l})$ and $(p_{s(r)l}, q_{s(r)l})$ later in this paper.

$$\text{Minimize}_{\Omega} f(\Omega) \quad (1a)$$

subject to

$$p_n - p_{d_n} = \sum_l (A_{nl}^+ p_{s_l} - A_{nl}^- p_{o_l}) + G_n V_n, \forall n \in \mathcal{N} \quad (1b)$$

$$q_n - q_{d_n} = \sum_l (A_{nl}^+ q_{s_l} - A_{nl}^- q_{o_l}) - B_n V_n, \forall n \in \mathcal{N} \quad (1c)$$

$$V_{s_l} - V_{r_l} = 2R_l p_{s_l} + 2X_l q_{s_l} - R_l p_{o_l} - X_l q_{o_l}, \forall l \in \mathcal{L} \quad (1d)$$

$$v_{s_l} v_{r_l} \sin \theta_l = X_l p_{s_l} - R_l q_{s_l}, \forall l \in \mathcal{L} \quad (1e)$$

$$i_{s(r)l}^2 = \frac{p_{s(r)l}^2 + q_{s(r)l}^2}{V_{s(r)l}^2} \leq K'_l, \forall l \in \mathcal{L} \quad (1f)$$

$$V_n = v_n^2, \forall n \in \mathcal{N} \quad (1g)$$

$$p_{o_l} = \frac{p_{s_l}^2 + q_{s_l}^2}{V_{s_l}} R_l \quad (1h) \quad q_{o_l} = \frac{p_{s_l}^2 + q_{s_l}^2}{V_{s_l}} X_l \quad (1i)$$

$$\theta_l \in [\theta_l^{min}, \theta_l^{max}], \quad v_n \in [v_n^{min}, v_n^{max}] \quad (1j)$$

$$p_n \in [p_n^{min}, p_n^{max}], \quad q_n \in [q_n^{min}, q_n^{max}] \quad (1k)$$

Where $\Omega = \{p_n, q_n, p_{s_l}, q_{s_l}, p_{o_l}, q_{o_l}, V_n, v_n, \theta_l\} \in \mathbb{R}^m$ is the set of model variables.² $n \in \mathcal{N}$ is the index of nodes. $l \in \mathcal{L}$ is the index of branches. Based on the applications, the objective function $f(\Omega)$ can be the economic cost of energy production or network power losses etc. In this paper, we assume the objective function is convex. Equations (1b) and (1c) represent the active and reactive power balance. G_n, B_n are the shunt conductance and susceptance of node n . A_{nl}^+ and A_{nl}^- are the node-to-branch incidence matrices of the network with $A_{nl}^+ = 1, A_{nl}^- = 0$ if n is the sending-end of branch l , and $A_{nl}^+ = -1, A_{nl}^- = -1$ if n is the receiving-end of branch l . p_n, q_n are the active and reactive power injections (generations) at node n . p_{d_n}, q_{d_n} are the active and reactive load absorptions of node n . V_n is the phase-to-ground voltage magnitude square at node n . p_{o_l}, q_{o_l} are the active and reactive power losses of branch l . Constraints (1b)-(1e) make the o-ACOPF model valid for both radial and meshed power networks. Equations (1d)-(1e) are derived by taking the magnitude and phase angle of the voltage drop phasor along branch l respectively. v_{s_l}, v_{r_l} are the sending- and receiving- end phase-to-ground voltage of branch l . $V_{s(r)_l} = v_{s(r)_l}^2$ are voltage magnitude squares. $\theta_l = \theta_{s_l} - \theta_{r_l}$ is the phase angle difference between sending- and receiving- end voltages of branch l . $\theta_{s_l}, \theta_{r_l}$ are the phase angles of sending- and receiving- end phase-to-ground voltages of branch l . To guarantee this derivation is valid, we assume $(\theta_l^{min}, \theta_l^{max}) \subseteq (-\frac{\pi}{2}, \frac{\pi}{2})$. i_{s_l}, i_{r_l} are the non-measurable sending- and receiving- end current flows of branch l . i'_{s_l}, i'_{r_l} are the measurable sending- and receiving- end current flows of branch l . K'_l is the actual ampacity of branch l which is provided from the branch manufacturer. Equations (1h)-(1i) represent active power and reactive power losses. Constraints (1j)-(1k) are bounds for voltage magnitude, voltage phase angle difference, nodal active power injection and nodal reactive power injection. p_n^{min}, p_n^{max} are the lower and upper bounds of p_n . q_n^{min}, q_n^{max} are the lower and upper bounds of q_n . $\theta_l^{min}, \theta_l^{max}$ are the lower and upper bounds of θ_l . This model is nonconvex because of the constraints (1e), (1g), (1h) and (1i). Current available nonlinear programming solvers are hard to efficiently find the global optimal solution of this nonconvex optimization model.

B. Second-Order Cone Relaxation

The SOC-ACOPF model is derived using branch sending-end power injections and voltage phase angle difference variables. Note that in the derived model, voltage square variables are included (voltage can be recovered from the model by taking the square root of the voltage square solutions). SOC-ACOPF is formulated in optimization model-(2). The numer-

ical performance of this model compared with other SOCP based ACOPF models can be found at [24].

$$\text{Minimize } f(\Omega) \quad (2a)$$

$$\text{subject to } (1b) - (1c), (1d), (1j) - (1k)$$

$$K_{o_l} \geq q_{o_l} \geq \frac{p_{s(r)_l}^2 + q_{s(r)_l}^2}{V_{s(r)_l}} X_l, \quad \forall l \in \mathcal{L} \quad (2b)$$

$$p_{o_l} X_l = q_{o_l} R_l, \quad \forall l \in \mathcal{L} \quad (2c)$$

$$\theta_l = X_l p_{s_l} - R_l q_{s_l}, \quad \forall l \in \mathcal{L} \quad (2d)$$

Constraints (2b)-(2c) represent active power and reactive power losses. K_{o_l} are the equivalent ampacity constraint for power losses of branch l . The left side of (2b) bounds q_{o_l} , which equivalently bounds the ampacity of branch l as explained in the next section. Equation (2d) is approximated from the nonconvex constraint (1e). This approximation is based on the assumption $v_{s_l} v_{r_l} \sin \theta_l \approx \theta_l$. The left side of equation (2d) can also be derived by the first-order Taylor series expansion of $v_{s_l} v_{r_l} \sin \theta_l$ for $v_{s_l} = v_{r_l} = 1$ and $\theta_l = 0$. We will show later that using (2d) actually relaxes the ACOPF model when $v_n \in (0.9, 1.1)$ and $\theta_l \in (-\frac{\pi}{2}, \frac{\pi}{2})$. It is worth to mention that even though constraint (2d) is the only constraint associated with the voltage phase angle variable, it should be solved jointly with other constraints in order to guarantee the feasibility of $\theta_l, p_{o_l}, q_{o_l}$.

III. DERIVING THE AMPACITY CONSTRAINT FOR THE POWER LOSSES

Since the actual measurable power flows (p'_{s_l}, q'_{s_l}) and current $i'_{s(r)_l}$ are different from the power flow variables (p_{s_l}, q_{s_l}) and $i_{s(r)_l}$ that we are using in the SOC-ACOPF model, it is necessary to derive the gap between $i'_{s(r)_l}$ and $i_{s(r)_l}$ to derive K_{o_l} according to the known parameter K'_l . From Fig. 1, we have:

$$p'_{s(r)_l} = p_{s(r)_l} \quad (3a)$$

$$q'_{s(r)_l} = q_{s(r)_l} - q_{cs(r)_l} \quad (3b)$$

$$q_{cs(r)_l} = V_{s(r)_l} B_{s(r)_l} \quad (3c)$$

Where $q_{cs(r)_l}$ is the reactive power injection from the sending-(receiving-) end shunt capacitance for the branch l , $B_{s(r)_l}$ is the shunt susceptance. The ampacity constraint of branch l is:

$$\|i'_{s(r)_l}\|^2 = \frac{p_{s(r)_l}^2 + q_{s(r)_l}^2}{V_{s(r)_l}} \leq K'_l \quad (3d)$$

From (3a)-(3d), we can derive the gap $\Delta^2 I$ between $\|i_{s(r)_l}\|^2$ and $\|i'_{s(r)_l}\|^2$:

$$\begin{aligned} \Delta^2 I &= \|i_{s(r)_l}\|^2 - \|i'_{s(r)_l}\|^2 = \frac{-q_{cs(r)_l}^2 + 2q_{s(r)_l} q_{cs(r)_l}}{V_{s(r)_l}} \\ &= \frac{-V_{s(r)_l}^2 B_{s(r)_l}^2 + 2q_{s(r)_l} V_{s(r)_l} B_{s(r)_l}}{V_{s(r)_l}} \\ &= -V_{s(r)_l} B_{s(r)_l}^2 + 2q_{s(r)_l} B_{s(r)_l} \end{aligned} \quad (3e)$$

²Note this is not the set of state variables. The state variables are $\{v_n, \theta_l\}$.

The branch ampacity constraint (3d) is equivalent to:

$$i_{s(r)l}^2 = \frac{p_{s(r)l}^2 + q_{s(r)l}^2}{V_{s(r)l}^2} \leq K_l = K_l' + \Delta^2 I \quad (3f)$$

The reactive power losses upper bounds K_{ol} can be quantified as:

$$K_{ol} = K_l X_l = (K_l' + \Delta^2 I) X_l \\ = (K_l' - V_{s(r)l} B_{s(r)l}^2 + 2q_{s(r)l} B_{s(r)l}) X_l \quad (3g)$$

Note equation (3g) is linear. So, if we use the expression of K_{ol} from (3g) in the constraint (2b), the SOC-ACOPF model-(2) is still convex and we avoid any approximation on the branch ampacity constraint.

It is worth to mention that using K_{ol} to constrain the upper bound of power losses p_{ol} in (2b) is more realistic than constraining the power flows (p_{s_l}, q_{s_l}) or (p_{s_l}, q_{s_l}) in the way of $p_{s_l}^{(')2} + q_{s_l}^{(')2} \leq S_l$ (where S_l is the maximum branch power flow). This is because:

- (i) the branch ampacity is given by the manufacturers in the form of maximum current $i_{s(r)l}^{max} = \sqrt{K_l'}$.
- (ii) the temperature increase of the branch (which lead to insulation degrading) is actually caused by the power losses due to the current which is the typical variable constrained by the branch manufacturer.
- (iii) the voltage amplitudes $v_{s(r)l}$ of both ends of the branch are varying during the grid operations. The maximum allowed power capacity $S_l = v_{s(r)l} i_{s(r)l}^{max}$ of the branch would then depend on the nodal voltage amplitudes at the branch ends.

IV. PROPERTIES OF THE SOC-ACOPF MODEL

Theorem 1

Assume $v_n \in (0.9, 1.1)$ and $\theta_l \in (-\frac{\pi}{2}, \frac{\pi}{2})$, replacing (1e) by (2d) relaxes the o-ACOPF model-(1) i.e. the SOC-ACOPF model-(2) is a relaxation of the o-ACOPF model-(1) (rather than an approximation of the o-ACOPF model).

Proof. We prove this theorem by showing that any point in the feasible region of o-ACOPF model-(1) can always map to a point located in the feasible region of the SOC-ACOPF model-(2). However, the reverse statement does not hold. In other words, some feasible solutions of the SOC-ACOPF model-(2) are not feasible for the o-ACOPF model-(1). Suppose $\Omega_0 = \{p_{0,n}, q_{0,n}, p_{0,s_l}, q_{0,s_l}, p_{0,o_l}, q_{0,o_l}, V_{0,n}, v_{0,n}, \theta_{0,l}\} \in \mathbb{R}^m$ is one feasible solution of the o-ACOPF model-(1). From (1e) we have:

$$v_{0,s_l} v_{0,r_l} \sin \theta_{0,l} = X_l p_{0,s_l} - R_l q_{0,s_l}, \quad \forall l \in \mathcal{L} \quad (4a)$$

We can map Ω_0 to a feasible solution $\Omega_1 = \{p_{1,n}, q_{1,n}, p_{1,s_l}, q_{1,s_l}, p_{1,o_l}, q_{1,o_l}, V_{1,n}, \theta_{1,l}\} \in \mathbb{R}^{m-n}$ of the SOC-ACOPF model-(2) as:

$$\{\Omega_1 \setminus \theta_{1,l}\} := \{\Omega_0 \setminus (\theta_{0,l}, v_{0,n})\} \quad (4b)$$

$$\theta_{1,l} := v_{0,s_l} v_{0,r_l} \sin \theta_{0,l}, \quad \forall l \in \mathcal{L} \quad (4c)$$

Since $v_{0,s_l} v_{0,r_l} \sin \theta_{0,l} \in (-1.21, 1.21) \subset (-\frac{\pi}{2}, \frac{\pi}{2})$, equation (4c) is always mappable. Note $\theta_{1,l}$ is not necessarily equal to

$\theta_{0,l}$. On the other hand, mapping Ω_1 to Ω_0 ($v_{0,s_l} v_{0,r_l} \sin \theta_{0,l} = \theta_{1,l}$) is not feasible when $\theta_{1,l} > 1.21$ or $\theta_{1,l} < -1.21$. \square

Theorem 1 shows that the feasible region of SOC-ACOPF model-(2) covers all the feasible region of o-ACOPF model-(1). It is worth to mention that the assumptions of $v_n \in (0.9, 1.1)$ and $\theta_l \in (-\frac{\pi}{2}, \frac{\pi}{2})$ are the practical operational requirements for power system. These assumptions can be relaxed to some degrees while Theorem 1 is still valid.

Theorem 2

If $(\theta_l^{min}, \theta_l^{max}) \subseteq (-\frac{\pi}{2}, \frac{\pi}{2})$ and $\theta_l^{min} = -\theta_l^{max}$, the necessary condition of recovering (mapping) a feasible solution of the o-ACOPF model-(1) from the (optimal) solution Ω_1 of SOC-ACOPF model-(2) is:

$$V_{s_l} V_{r_l} \sin^2(\theta_l^{max}) \geq \theta_l^2, \quad \forall l \in \mathcal{L} \quad (4d)$$

Note constraint (4d) is conic and thus convex.

Proof. If a feasible solution Ω_0 of the o-ACOPF model-(1) is recovered (mapped) from the (optimal) solution Ω_1 of the SOC-ACOPF model-(2):

$$\{\Omega_0 \setminus (\theta_{0,l}, v_{1,n})\} := \{\Omega_1 \setminus (\theta_{1,l})\} \quad (4e)$$

$$v_{0,n} := \sqrt{V_{1,n}}, \quad \forall n \in N \quad (4f)$$

$$\theta_{0,l} := \arcsin\left(\frac{X_l p_{s_{1,l}} - R_l q_{s_{1,l}}}{v_{1,s_l} v_{1,r_l}}\right) \\ = \arcsin\left(\frac{\theta_{1,l}}{v_{1,s_l} v_{1,r_l}}\right), \quad \forall l \in \mathcal{L} \quad (4g)$$

Since $\sin(\theta_{1,l})$ is monotonic in $(\theta_l^{min}, \theta_l^{max}) \subseteq (-\frac{\pi}{2}, \frac{\pi}{2})$, equation (4g) implies:

$$\sin(\theta_l^{min}) \leq \frac{\theta_{1,l}}{v_{s_{1,l}} v_{r_{1,l}}} \leq \sin(\theta_l^{max}), \quad \forall l \in \mathcal{L} \quad (4h)$$

Considering $\sin^2(\theta_l^{min}) = \sin^2(\theta_l^{max})$ when $\theta_l^{min} = -\theta_l^{max}$, constraint (4h) is equivalent to:

$$\frac{\theta_{1,l}^2}{V_{s_l} V_{r_l} \sin^2(\theta_l^{max})} \leq 1, \quad \forall l \in \mathcal{L} \quad (4i)$$

Or equivalently, $V_{s_{1,l}} V_{r_{1,l}} \sin^2(\theta_l^{max}) \geq \theta_{1,l}^2$. \square

Theorem 2 shows that if we add the convex constraint (4d) to the SOC-ACOPF model-(2), we can improve the solution feasibility towards the o-ACOPF model-(1). Please note that equations (4e)-(4g) is only one way to recover the feasible solution. Condition (4d) is necessary to recover the feasible solution by using this approach. There can be other feasible solution recovery approaches which do not require condition (4d).

Theorem 3

The SOC-ACOPF model-(2) with the additional constraint (4d) is a relaxation of the o-ACOPF model-(1).

Proof. We can use the same procedure in proving theorem 1 to prove theorem 3 i.e. any feasible solution of the o-ACOPF model-(1) can be mapped to a feasible solution of the SOC-ACOPF model-(2) with additional constraint (4d). However, the reverse statement is not true when there is at least one $\hat{l} \in \mathcal{L}$ (in the feasible solution of the SOC-ACOPF model-(2) with

the additional constraint (4d)) such that $q_{o_i} > \frac{p_{s(r)_i}^2 + q_{s(r)_i}^2}{V_{s(r)_i}} X_i$ (which fails to satisfy constraints (1i) in the o-ACOPF model-(1) obviously). \square

Theorem 3 shows that the SOC-ACOPF model-(2) with the additional constraint (4d) still covers the feasible region of the o-ACOPF model-(1).

Theorem 4

If the optimal solution Ω^* of the SOC-ACOPF model-(2) with additional constraint (4d) gives tight relaxation $q_{o_i}^* = \frac{p_{s(r)_i}^2 + q_{s(r)_i}^2}{V_{s(r)_i}} X_i, \forall i \in L$, the global optimal solution Ω_0^* of the o-ACOPF model-(1) is $\Omega_0^* := \{\Omega^* \setminus \theta_i^*\} \cup \{v_{0,n}^* := \sqrt{V_n^*}, \theta_{0,l}^* := \arcsin(\frac{\theta_l^*}{v_{s_l}^* v_{r_l}^*})\}$.

Proof. Theorem 4 is a direct result of theorem 1, theorem 2 and theorem 3 considering the optimal objective solution f^* of the SOC-ACOPF model-(2) is always a lower bound for the optimal objective solution f_0^* of the o-ACOPF model-(1). \square

Theorem 5

Define the (parametric) optimal value functions:

$$f^*(p_{d_n}, q_{d_n}) := \min f(\Omega, p_{d_n}, q_{d_n}) \text{ s.t. } \{\Omega \in \Omega_{ACOPF}\} \quad (4j)$$

$$f^*(p_{d_n}, q_{d_n}) := \min f(\Omega, p_{d_n}, q_{d_n}) \text{ s.t. } \{\Omega \in \Omega_{SOC-ACOPF}\} \quad (4k)$$

Where Ω_{ACOPF} and $\Omega_{SOC-ACOPF}$ are the feasible regions of the o-ACOPF model-(1) and SOC-ACOPF model-(2) correspondingly. If the objective function f is a monotonically increasing function of (p_n, q_n) i.e. $f(p_{1,n}, q_{1,n}) \leq f(p_{2,n}, q_{2,n})$ for $(p_{1,n}, q_{1,n}) \leq (p_{2,n}, q_{2,n})$, the optimal value functions f^* are monotonic i.e. $f^*(p_{d_{1,n}}, q_{d_{1,n}}) \leq f^*(p_{d_{2,n}}, q_{d_{2,n}})$ if $(p_{d_{1,n}}, q_{d_{1,n}}) \leq (p_{d_{2,n}}, q_{d_{2,n}})$ (assuming the o-ACOPF and SOC-ACOPF models are feasible for $(p_{d_{1,n}}, q_{d_{1,n}})$ and $(p_{d_{2,n}}, q_{d_{2,n}})$).

Proof. We prove theorem 5 by contradiction. Suppose the optimal solutions and objectives of the SOC-ACOPF (or o-ACOPF) model at $(p_{d_{1,n}}, q_{d_{1,n}})$ and $(p_{d_{2,n}}, q_{d_{2,n}})$ are $\Omega_1^* = \{p_{1,n}^*, q_{1,n}^*, p_{1,s_l}^*, q_{1,s_l}^*, p_{1,o_l}^*, q_{1,o_l}^*, V_{1,n}^*, \theta_{1,l}^*\} \in \mathbb{R}^{m-n}, f_1^*$ and $\Omega_2^* = \{p_{2,n}^*, q_{2,n}^*, p_{2,s_l}^*, q_{2,s_l}^*, p_{2,o_l}^*, q_{2,o_l}^*, V_{2,n}^*, \theta_{2,l}^*\} \in \mathbb{R}^{m-n}, f_2^*$. If $f_1^* > f_2^*$ for $(p_{d_{1,n}}, q_{d_{1,n}}) \leq (p_{d_{2,n}}, q_{d_{2,n}})$, since f is monotonic, there must be at least one $\hat{n} \in N$ such that $(p_{1,\hat{n}}^*, q_{1,\hat{n}}^*) > (p_{2,\hat{n}}^*, q_{2,\hat{n}}^*)$. We can construct a feasible solution Ω_1' of the SOC-ACOPF (or o-ACOPF) model at $(p_{d_{1,n}}, q_{d_{1,n}})$ (by using Ω_2^*) as:

$$\{\Omega_1' \setminus (p_{1,\hat{n}}', q_{1,\hat{n}}')\} := \{\Omega_2^* \setminus (p_{2,\hat{n}}^*, q_{2,\hat{n}}^*)\} \quad (4l)$$

From (1b)-(1c), we have:

$$p_{2,\hat{n}}^* - p_{d_{2,\hat{n}}} = \sum_l (A_{\hat{n}l}^+ p_{s_{2,l}}^* - A_{\hat{n}l}^- p_{o_{2,l}}^*) + G_{\hat{n}} V_{2,\hat{n}}^* \quad (4m)$$

$$q_{2,\hat{n}}^* - q_{d_{2,\hat{n}}} = \sum_l (A_{\hat{n}l}^+ q_{s_{2,l}}^* - A_{\hat{n}l}^- q_{o_{2,l}}^*) - B_{\hat{n}} V_{2,\hat{n}}^* \quad (4n)$$

We know the feasible solution of $(p_{1,\hat{n}}, q_{1,\hat{n}})$ must satisfy:

$$p_{1,\hat{n}}' - p_{d_{1,\hat{n}}} = \sum_l (A_{\hat{n}l}^+ p_{s_{2,l}}^* - A_{\hat{n}l}^- p_{o_{2,l}}^*) + G_{\hat{n}} V_{2,\hat{n}}^* \quad (4o)$$

$$q_{1,\hat{n}}' - q_{d_{1,\hat{n}}} = \sum_l (A_{\hat{n}l}^+ q_{s_{2,l}}^* - A_{\hat{n}l}^- q_{o_{2,l}}^*) - B_{\hat{n}} V_{2,\hat{n}}^* \quad (4p)$$

Substituting (4o)-(4p) to (4m)-(4n), we have:

$$p_{1,\hat{n}}' - p_{d_{1,\hat{n}}} = p_{2,\hat{n}}^* - p_{d_{2,\hat{n}}} \quad (4q)$$

$$q_{1,\hat{n}}' - q_{d_{1,\hat{n}}} = q_{2,\hat{n}}^* - q_{d_{2,\hat{n}}} \quad (4r)$$

$$\text{Which yield: } p_{1,\hat{n}}' = p_{2,\hat{n}}^* + p_{d_{1,\hat{n}}} - p_{d_{2,\hat{n}}} \quad (4s)$$

$$q_{1,\hat{n}}' = q_{2,\hat{n}}^* + q_{d_{1,\hat{n}}} - q_{d_{2,\hat{n}}} \quad (4t)$$

So $\Omega_1' = \{\Omega_2^* \setminus (p_{2,\hat{n}}^*, q_{2,\hat{n}}^*)\} \cup (p_{1,\hat{n}}', q_{1,\hat{n}}')$ is feasible for the SOC-ACOPF (or o-ACOPF) model. Because $(p_{d_{1,n}}, q_{d_{1,n}}) \leq (p_{d_{2,n}}, q_{d_{2,n}})$, equations (4s)-(4t) imply $(p_{1,\hat{n}}', q_{1,\hat{n}}') \leq (p_{2,\hat{n}}^*, q_{2,\hat{n}}^*)$. This means the corresponding objective function value $f_1' \leq f_2^* < f_1^*$ (note $(p_{1,n}', q_{1,n}') = (p_{2,n}^*, q_{2,n}^*) \forall n \neq \hat{n}$) which contradicts the assumption that f_1^* is the optimal objective solution. So $f_1^* > f_2^*$ cannot hold for $(p_{d_{1,n}}, q_{d_{1,n}}) \leq (p_{d_{2,n}}, q_{d_{2,n}})$. This completes the proof. \square

Theorem 6

Assuming $(\theta_l^{min}, \theta_l^{max}) \subseteq (-\frac{\pi}{2}, \frac{\pi}{2})$ and the objective function f is monotonically increasing for (p_n, q_n) , if the optimal solution Ω^* of the SOC-ACOPF model-(2) (with additional constraint (4d)) at (p_{d_n}, q_{d_n}) has positive relaxation gap $q_{o_i}^* > \frac{p_{s(r)_i}^2 + q_{s(r)_i}^2}{V_{s(r)_i}} X_i$ or $p_{o_i}^* > \frac{p_{s(r)_i}^2 + q_{s(r)_i}^2}{V_{s(r)_i}} R_i$ for some $\hat{l} \in \mathcal{L}$, there exists $(p_{d_n}', q_{d_n}') > (p_{d_n}, q_{d_n})$ at which the relaxation is tight for the optimal solution i.e. $q_{o_l}^* = \frac{p_{s(r)_l}^2 + q_{s(r)_l}^2}{V_{s(r)_l}} X_l \forall l \in \mathcal{L}$ or $p_{o_i}^* = \frac{p_{s(r)_i}^2 + q_{s(r)_i}^2}{V_{s(r)_i}} R_i$.

Proof. To prove theorem 6, we firstly derive an equivalent model of the o-ACOPF model-(1) by replacing constraint (1d) with:

$$V_{s_l} - v_{s_l} v_{r_l} \cos \theta_l = p_{s_l} R_l + q_{s_l} X_l, \forall l \in \mathcal{L} \quad (4u)$$

Constraints (4u)-and-(1e) are equivalent with constraints (1d)-and-(1e) for $(\theta_l^{min}, \theta_l^{max}) \subseteq (-\frac{\pi}{2}, \frac{\pi}{2})$ since they are expressing the same voltage drop phasor either in the way of real-and-imaginary parts or amplitude-and-imaginary parts illustrated in Fig. 2. We then define a new relaxed ACOPF model as

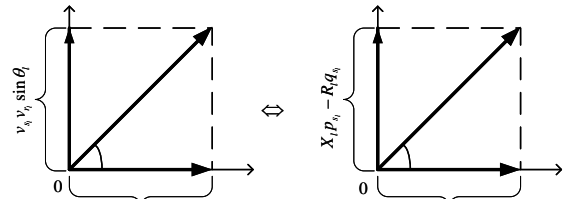


Fig. 2. Equivalent constraint of the Branch Voltage Drop Phasor

r-ACOPF in (4v).

$$\text{Minimize } f(\Omega) \quad (4v)$$

subject to (1b) – (1c), (1e), (1g), (1j) – (1k), (2b) – (2c), (4u)

Obviously, when the relaxation is tight, the feasible region of the r-ACOPF model-(4v) is actually equivalent to the feasible region of the SOC-ACOPF model-(2) (with additional constraint (4d)) since any feasible solution from either model (r-ACOPF or SOC-ACOPF) can be mapped to the feasible region of another model (SOC-ACOPF or r-ACOPF) using the procedures we derived in theorems 1-4. The feasible region comparison is shown in Fig. 3.

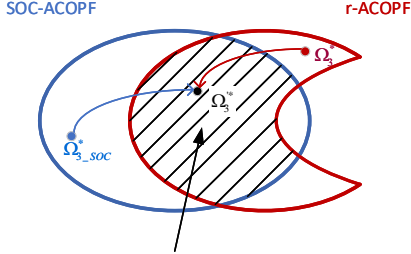


Fig. 3. Comparison of the Feasible Regions of SOC-ACOPF and r-ACOPF

We want to emphasize here that, although the r-ACOPF model-(4v) is nonconvex (with regarding to its own set of variables), it is valid that part of its feasible region can be mapped to a convex one (with another set of variables) such as the convex SOC-ACOPF model-(2) (with additional constraint (4d)). A obvious simple example is the equivalence between the nonconvex region expressed by $\{y = x^2, x > 0\}$ for $(y, x) \in \mathbb{R}$ and convex region expressed by $\{y = z, z > 0\}$ for $(y, z) \in \mathbb{R}$. Fig. 4 shows this equivalence graphically. A similar consideration can be drawn for the r-ACOPF model-(4v) (where both $V_n = v_n^2$ and v_n are deployed) and the SOC-ACOPF model-(2) where only V_n are used.

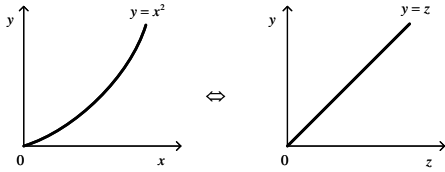


Fig. 4. The Equivalence of Regions Expressed by Different Variables

Similarly, we define the (parametric) optimal value function of the r-ACOPF model-(4v) (with regarding to (p_{d_n}, q_{d_n})) as:

$$f^*(p_{d_n}, q_{d_n}) := \min f(\Omega, p_{d_n}, q_{d_n}) \quad s.t. \quad \{\Omega \in \Omega_{r-ACOPF}\} \quad (4w)$$

Following the same procedure in the proof of theorem 5, it is obvious that f^* here is also monotonic.

We now use the r-ACOPF model-(4v) as a bridge to prove theorem 6. The key procedure is to show that theorem 6 is valid for the r-ACOPF model-(4v) and thus valid for the SOC-ACOPF model-(2) considering the equivalence between their feasible regions (when the relaxation is tight). Suppose the optimal solution Ω_3^* of the r-ACOPF model-(4v) has positive relaxation gap $q_{o3,\hat{l}}^* > \frac{p_{3,s(r)\hat{l}}^{*2} + q_{3,s(r)\hat{l}}^{*2}}{V_{3,s(r)\hat{l}}^*} X_{\hat{l}}$ or

$$p_{o3,\hat{l}}^* > \frac{p_{3,s(r)\hat{l}}^{*2} + q_{3,s(r)\hat{l}}^{*2}}{V_{3,s(r)\hat{l}}^*} R_{\hat{l}} \text{ for some } \hat{l} \in \mathcal{L} \text{ at } (p_{d_n}, q_{d_n}), \text{ we}$$

use $\Delta^* p_{o3,\hat{l}} > 0$ and $\Delta^* q_{o3,\hat{l}} > 0$ to represent the active and reactive power losses relaxation gaps respectively:

$$p_{o3,\hat{l}}^* - \frac{p_{3,s(r)\hat{l}}^{*2} + q_{3,s(r)\hat{l}}^{*2}}{V_{3,s(r)\hat{l}}^*} R_{\hat{l}} = \Delta^* p_{o3,\hat{l}} \quad (4x)$$

$$q_{o3,\hat{l}}^* - \frac{p_{3,s(r)\hat{l}}^{*2} + q_{3,s(r)\hat{l}}^{*2}}{V_{3,s(r)\hat{l}}^*} X_{\hat{l}} = \Delta^* q_{o3,\hat{l}} \quad (4y)$$

So the tight power losses solutions are $p_{o3,\hat{l}}' = p_{o3,\hat{l}}^* - \Delta^* p_{o3,\hat{l}} > 0$ and $q_{o3,\hat{l}}' = q_{o3,\hat{l}}^* - \Delta^* q_{o3,\hat{l}} > 0$. From constraints (1b)-(1c), we have:

$$p_{3,n}^* - p_{d_n} = \sum_l (A_{nl}^+ p_{s3,l}^* - A_{nl}^- p_{o3,l}^*) + G_n V_{3,n}^* \quad (4z)$$

$$q_{3,n}^* - q_{d_n} = \sum_l (A_{nl}^+ q_{s3,l}^* - A_{nl}^- q_{o3,l}^*) - B_n V_{3,n}^* \quad (4aa)$$

Suppose at (p_{d_n}', q_{d_n}') , tight power losses solutions are found (note in the r-ACOPF model only following constraints are associated with the power losses variables aside from constraints (2b)-(2c)):

$$p_{3,n}^* - p_{d_n}' = \sum_l (A_{nl}^+ p_{s3,l}^* - A_{nl}^- p_{o3,l}^*) + G_n V_{3,n}^* \quad (4ab)$$

$$q_{3,n}^* - q_{d_n}' = \sum_l (A_{nl}^+ q_{s3,l}^* - A_{nl}^- q_{o3,l}^*) - B_n V_{3,n}^* \quad (4ac)$$

Combining equations (4z)-(4aa) with equations (4ab)-(4ac), we have:

$$p_{d_n}' = p_{d_n} - \sum_l A_{nl}^- \Delta^* p_{o3,l}^* \quad (4ad)$$

$$q_{d_n}' = q_{d_n} - \sum_l A_{nl}^- \Delta^* q_{o3,l}^* \quad (4ae)$$

Because $A_{nl}^- \in \{0, -1\}$ and $(\Delta^* p_{o3,l}^*, \Delta^* q_{o3,l}^*) > 0$, equations (4ad)-(4ae) imply $(p_{d_n}', q_{d_n}') > (p_{d_n}, q_{d_n})$. Taking into account that the optimal value function f^* is monotonic, we also know that $f^*(p_{d_n}, q_{d_n}) < f^*(p_{d_n}', q_{d_n}')$ which means Ω^* is not only feasible but also optimal for the r-ACOPF model-(4v) at (p_{d_n}', q_{d_n}') . As we have explained at the beginning of this proof, since the r-ACOPF model-(4v) is actually equivalent (in terms of the feasible region and optimal solution when the relaxation is tight) with the SOC-ACOPF model-(2), all the tight solutions we derived in proving theorem 6 for the r-ACOPF model-(4v) can always be mapped to the corresponding tight solution of the SOC-ACOPF model-(2). In other words, theorem 6 is also valid for the SOC-ACOPF model-(2). \square

Theorem 6 shows the structure of the relaxed solutions and tight solutions for the SOC-ACOPF model-(2) with regarding to the load absorption parameter. This theorem shows a counter-intuitive property of the SOC-ACOPF model-(2) that larger power load can help tighten the relaxation gap. We present in the next section the numerical validations of all the theorems and analysis in this section.

TABLE I
OBJECTIVE SOLUTIONS

Test case	10% Load		20% Load		30% Load		40% Load	
	SOC-ACOPF	o-ACOPF	SOC-ACOPF	o-ACOPF	SOC-ACOPF	o-ACOPF	SOC-ACOPF	o-ACOPF
IEEE14	545.64	546.37	1147.21	1147.50	1806.10	1806.26	2523.77	2523.91
case30	33.14	33.14	75.31	75.31	123.61	123.61	178.12	178.12
IEEE57	2682.55	2686.41	5706.04	5709.00	9080.48	9082.93	12809.00	12810.65
IEEE118	8940.49	8952.62	18735.71	18750.11	29420.72	29436.19	41008.27	41025.36
ACTIVSg200	14070.44	14070.44	14070.44	14070.44	14070.44	14070.44	14483.45	14483.82
IEEE300	51210.16	56915.23	107284.01	108378.18	168588.72	168712.09	235157.51	235244.97
ACTIVSg500	16386.94	16386.94	16386.94	16386.94	16386.94	16386.94	16386.94	16386.94
1354pegase	7558.35	7558.47	15101.85	15102.06	22665.28	22665.88	30246.88	30249.40
2869pegase	14639.05	14754.46	29204.10	29236.82	43811.78	43830.34	58458.84	58467.05

TABLE II
MAXIMUM RELAXATION GAPS OF ACTIVE POWER LOSSES FROM THE SOC-ACOPF MODEL

Test case	10% Load	>10% Load	20% Load	>20% Load	30% Load	>30% Load	40% Load	>40% Load
IEEE14	5.43E-10	7.31E-13	3.35E-09	6.89E-13	1.06E-10	6.85E-12	2.99E-09	1.45E-12
case30	5.45E-10	6.47E-10	1.67E-10	1.33E-11	1.71E-09	1.72E-10	1.21E-10	1.84E-10
IEEE57	1.84E-10	5.92E-10	2.52E-11	7.46E-10	1.36E-09	2.09E-10	6.38E-09	8.26E-10
IEEE118	4.93E-09	3.28E-09	6.02E-08	1.79E-09	1.11E-07	1.10E-09	1.57E-09	3.99E-11
ACTIVSg200	1.67E-02	1.28E-10	1.43E-02	3.37E-10	6.65E-03	6.97E-10	1.45E-08	5.79E-10
IEEE300	1.15E-02	4.14E-08	1.37E-03	8.17E-09	4.08E-06	2.52E-09	5.01E-05	1.10E-09
ACTIVSg500	2.29E-02	1.34E-09	2.12E-02	3.69E-09	1.93E-02	5.49E-10	1.60E-02	3.59E-10
1354pegase	3.09E-03	1.79E-07	2.72E-07	1.42E-07	1.01E-02	1.43E-07	1.04E-02	1.03E-07
2869pegase	8.47E-03	7.12E-06	9.32E-03	1.38E-07	6.72E-03	6.56E-08	1.47E-02	6.99E-08

TABLE III
MAXIMUM RELAXATION GAPS OF REACTIVE POWER LOSSES FROM THE SOC-ACOPF MODEL

Test case	10% Load	>10% Load	20% Load	>20% Load	30% Load	>30% Load	40% Load	>40% Load
IEEE14	2.50E-01	8.51E-11	7.95E-02	3.92E-11	1.43E-01	1.24E-10	1.18E-01	2.33E-11
case30	2.31E-02	1.78E-09	2.34E-02	2.65E-11	2.21E-02	3.66E-10	2.04E-02	3.79E-10
IEEE57	2.25E-01	2.00E-09	1.92E-01	9.65E-09	1.46E-01	3.10E-09	1.02E-01	3.37E-09
IEEE118	2.98E+00	1.00E-08	3.08E+00	1.37E-08	2.86E+00	9.55E-09	2.84E+00	3.03E-09
ACTIVSg200	2.05E-01	1.35E-09	1.99E-01	1.94E-09	2.09E-01	7.14E-09	1.06E-06	2.91E-09
IEEE300	5.25E+00	9.33E-08	4.12E+00	1.75E-08	3.82E+00	3.26E-08	3.62E+00	6.55E-08
ACTIVSg500	3.31E-01	1.41E-08	2.87E-01	4.88E-08	2.45E-01	7.27E-09	2.33E-01	4.74E-09
1354pegase	2.95E-01	1.46E-06	2.93E-01	3.45E-07	8.50E-01	4.77E-07	8.74E-01	2.63E-07
2869pegase	7.81E-01	4.96E-05	5.03E-01	3.44E-06	3.79E-01	8.79E-07	2.64E+00	1.12E-06

V. NUMERICAL RESULTS AND DISCUSSION

The SOC-ACOPF model-(2) and o-ACOPF model-(1) are implemented in the YALMIP [25] toolbox for modelling and optimization in MATLAB running on the 64-bit macOS operating system. A personal computer with Intel Core i9 2.9 GHz CPU and 16G RAM is deployed. The MOSEK and SCS solvers are used to solve the SOC-ACOPF model-(2). Because MOSEK and SCS can only solve convex models, the convexity of the SOC-ACOPF model-(2) is numerically validated. The IPOPT solver is used to solve the nonconvex o-ACOPF model-(1). We use IEEE networks {14, 57, 118, 300}, matpower case30, ACTIVSg {200, 500} and {1354, 2869} pegase [26] test cases to validate our proposed theorems in this Section. Power network data from MATPOWER are directly used here [27]. The objective function f of typical economic dispatch is quadratic i.e. $f(p_n) = \sum_n \alpha_n p_n^2 + \beta_n p_n + \gamma_n$. Where $(\alpha_n, \beta_n, \gamma_n) \geq 0$ are the cost parameters of nodal active power generation. Note some cost parameters are equal to zero in the test cases. To make sure the objective function f is monotonic for p_n , we must ensure $p_n^{min} \geq 0$ in the o-ACOPF and SOC-ACOPF models.

Since we have tested our models for the base load and shown in our previous work [24] that large relaxation gaps

are present for optimal solutions in low load levels, we only show the results for low load levels here. In Table I, we list the objective solutions of the SOC-ACOPF model-(2) and the o-ACOPF model-(1) for 10%, 20%, 30% and 40% of the absolute value of base load. So, the results in Table I validate two of our theorems: (i) SOC-ACOPF model-(2) is a relaxation of the o-ACOPF model-(1). This is validated since all the objective solutions of the SOC-ACOPF model-(2) are lower than the o-ACOPF model-(1); (ii) the optimal value functions of the SOC-ACOPF model-(2) and the o-ACOPF model-(1) are monotonic (with regarding to power load p_d) given that the objective function f is monotonic with regarding to p_n . This is validated since all the objective solutions increase when the power load levels increase. For the SOC-ACOPF model-(2), the relaxation gaps of active power losses and reactive power losses are defined as:

$$Gap_l^{po} = p_{o_l} - \frac{p_{s_l}^2 + q_{s_l}^2}{V_{s_l}} R_l, \quad Gap_l^{qo} = q_{o_l} - \frac{p_{s_l}^2 + q_{s_l}^2}{V_{s_l}} X_l$$

The maximum relaxation gaps (of active and reactive power losses) are defined as $Gap^{po,max} = \text{Maximum}\{Gap_l^{po}, \forall l \in \mathcal{L}\}$ and $Gap^{qo,max} = \text{Maximum}\{Gap_l^{qo}, \forall l \in \mathcal{L}\}$. We use $Gap^{po,max}$ and $Gap^{qo,max}$ to measure the the relaxation performance of the

SOC-ACOPF model-(2) (smaller relaxation gaps mean better performance). We list the maximum relaxation gaps results $Gap^{po,max}$ and $Gap^{go,max}$ of the SOC-ACOPF model-(2) in Table II and Table III. When the relaxation is not tight, we increase the power load levels (p_d, q_d) (but fix the optimal nodal power injection solution p_n^* so the objective solutions remain the same as in Table I) to find the tight solutions of the SOC-ACOPF model-(2). The power load levels are increased by taking the power loads p_d, q_d as variables in the SOC-ACOPF model and using the original power load levels (10%, 20%, 30% and 40%) as the lower bounds of these variables. The maximum relaxation gaps for tight solutions are listed in the columns denoted as '>10% Load', '> 20% Load', '> 30% Load' and '> 40% Load' of Table II and Table III. So we have actually numerically validated theorem 6 by the results in Table II and Table III. It is worth to mention that for most branches, the relaxation gaps are very small. The maximum relaxation gap only appear for single branch in each test case.

VI. CONCLUSIONS

By equivalently deriving the branch ampacity constraint for the power losses, we firstly fill the approximation gap of the SOC-ACOPF model-(2) based on the branch flow formulation. We then give the analytical and numerical proofs for several important properties of the SOC-ACOPF model-(2). The aims of proving these properties are to improve the solution quality and to promote the applicability of the SOC-ACOPF model-(2). We show rigorously that the feasible region of the SOC-ACOPF model-(2) covers the feasible region of the o-ACOPF model-(1). Regarding to the AC feasibility of the solution from the SOC-ACOPF model-(2), one additional necessary conic constraint to improve the AC feasibility of the solution is derived in theorem 2. We also show how to recover the global optimal solution of the o-ACOPF model-(1) from the tight optimal solution of the SOC-ACOPF model-(2) in theorem 4. Based on the monotonic property of the optimal value functions defined by the SOC-ACOPF model-(2) and the o-ACOPF model (1) from theorem 5, we prove that the tight solutions of the SOC-ACOPF model-(2) can always be obtained by allowing the increase of nodal load absorptions in theorem 6. This theorem shows that large power load levels actually help tighten the relaxation gap of the SOC-ACOPF model-(2). In other words, SOC-ACOPF model-(2) is more applicable for high power load conditions.

REFERENCES

- [1] J. Carpentier, "Contribution to the economic dispatch problem," *Bulletin of the French Society of Electricians*, vol. 3, no. 8, pp. 431–447, 1962.
- [2] M. B. Cain, R. P. O'Neill, and A. Castillo, "History of optimal power flow and formulations," FERC, Tech. Rep., 2012.
- [3] P. Panciatici, M. C. Campi, S. Garatti, S. H. Low, D. K. Molzahn, A. X. Sun, and L. Wehenkel, "Advanced optimization methods for power systems," in *2014 Power Systems Computation Conference*, Aug 2014, pp. 1–18.
- [4] M. Farivar and S. H. Low, "Branch Flow Model: Relaxations and Convexification: Part I, Part II," *IEEE Transactions on Power Systems*, vol. 28, no. 3, pp. 2554–2572, Aug 2013.
- [5] L. Gan, N. Li, U. Topcu, and S. H. Low, "Exact convex relaxation of optimal power flow in radial networks," *Automatic Control, IEEE Transactions on*, vol. 60, no. 1, pp. 72–87, 2015.

- [6] B. Kocuk, S. S. Dey, and X. A. Sun, "Strong socp relaxations for the optimal power flow problem," *Operations Research*, vol. 64, pp. 1177–1196, 2016.
- [7] X. Bai, H. Wei, K. Fujisawa, and Y. Wang, "Semidefinite programming for optimal power flow problems," *International Journal of Electrical Power & Energy Systems*, vol. 30, no. 6, pp. 383–392, 2008.
- [8] J. Lavaei and S. H. Low, "Zero duality gap in optimal power flow problem," *Power Systems, IEEE Transactions on*, vol. 27, no. 1, pp. 92–107, 2012.
- [9] D. K. Molzahn and I. A. Hiskens, "Moment-based relaxation of the optimal power flow problem," in *2014 Power Systems Computation Conference*, Aug 2014, pp. 1–7.
- [10] —, "Sparsity-exploiting moment-based relaxations of the optimal power flow problem," *IEEE Transactions on Power Systems*, vol. 30, no. 6, pp. 3168–3180, Nov 2015.
- [11] H. Hijazi, C. Coffrin, and P. V. Hentenryck, "Convex quadratic relaxations for mixed-integer nonlinear programs in power systems," *Mathematical Programming Computation*, vol. 9, no. 3, pp. 321–367, Sep 2017.
- [12] C. Coffrin, H. L. Hijazi, and P. V. Hentenryck, "The QC Relaxation: A Theoretical and Computational Study on Optimal Power Flow," *IEEE Transactions on Power Systems*, vol. 31, no. 4, pp. 3008–3018, July 2016.
- [13] C. Coffrin, H. L. Hijazi, and P. Van Hentenryck, "Strengthening convex relaxations with bound tightening for power network optimization," in *Principles and Practice of Constraint Programming*, G. Pesant, Ed. Cham: Springer International Publishing, 2015, pp. 39–57.
- [14] M. Bynum, A. Castillo, J. Watson, and C. D. Laird, "Tightening McCormick relaxations toward global solution of the acopf problem," *IEEE Transactions on Power Systems*, vol. 34, no. 1, pp. 814–817, Jan 2019.
- [15] M. E. Baran and F. F. Wu, "Optimal capacitor placement on radial distribution systems," *IEEE Transactions on Power Delivery*, vol. 4, no. 1, pp. 725–734, Jan 1989.
- [16] R. Jabr *et al.*, "Radial distribution load flow using conic programming," *Power Systems, IEEE Transactions on*, vol. 21, no. 3, pp. 1458–1459, 2006.
- [17] K. Christakou, D.-C. Tomozei, J.-Y. L. B. Boudec, and M. Paolone, "AC OPF in Radial Distribution Networks-Parts I, II," *Electric Power Systems Research*, vol. 143, 150, pp. 438 – 450, 24–35, 2017.
- [18] M. Nick, R. Cherkaoui, J. L. Boudec, and M. Paolone, "An exact convex formulation of the optimal power flow in radial distribution networks including transverse components," *IEEE Transactions on Automatic Control*, vol. 63, no. 3, pp. 682–697, March 2018.
- [19] R. Madani, S. Sojoudi, and J. Lavaei, "Convex relaxation for optimal power flow problem: Mesh networks," *IEEE Transactions on Power Systems*, vol. 30, no. 1, pp. 199–211, Jan 2015.
- [20] A. Eltvad, J. Dahl, and M. S. Andersen, "On the robustness and scalability of semidefinite relaxation for optimal power flow problems," *Optimization and Engineering*, Mar 2019. [Online]. Available: <https://doi.org/10.1007/s11081-019-09427-4>
- [21] D. Shchetinin, T. A. Tinoco De Rubira, and G. Hug-Glanzmann, "Efficient bound tightening techniques for convex relaxations of ac optimal power flow," *IEEE Transactions on Power Systems*, pp. 1–1, 2019.
- [22] D. Shchetinin, T. T. De Rubira, and G. Hug, "On the construction of linear approximations of line flow constraints for ac optimal power flow," *IEEE Transactions on Power Systems*, vol. 34, no. 2, pp. 1182–1192, March 2019.
- [23] Z. Yuan, M. R. Hesamzadeh, and D. Biggar, "Distribution locational marginal pricing by convexified ACOPF and hierarchical dispatch," *IEEE Transactions on Smart Grid*, vol. PP, no. 99, pp. 1–1, 2016.
- [24] Z. Yuan and M. R. Hesamzadeh, "Second-order cone AC optimal power flow: convex relaxations and feasible solutions," *Journal of Modern Power Systems and Clean Energy*, vol. 7, no. 2, pp. 268–280, Mar 2019.
- [25] J. Löfberg, "Yalmip : A toolbox for modeling and optimization in matlab," in *In Proceedings of the CACSD Conference*, Taipei, Taiwan, 2004.
- [26] S. Fliscounakis, P. Panciatici, F. Capitanescu, and L. Wehenkel, "Contingency ranking with respect to overloads in very large power systems taking into account uncertainty, preventive, and corrective actions," *IEEE Transactions on Power Systems*, vol. 28, no. 4, pp. 4909–4917, Nov 2013.
- [27] R. D. Zimmerman, C. E. Murillo-Sánchez, and R. J. Thomas, "Matpower: Steady-state operations, planning, and analysis tools for power systems research and education," *Power Systems, IEEE Transactions on*, vol. 26, no. 1, pp. 12–19, 2011.